IOPscience iopscience.iop.org

Home Search Collections Journals About Contact us My IOPscience

Asymmetry in polariton dispersion as function of light and matter frequencies in the ultrastrong coupling regime

This content has been downloaded from IOPscience. Please scroll down to see the full text.

2017 New J. Phys. 19 043022

(http://iopscience.iop.org/1367-2630/19/4/043022)

View the table of contents for this issue, or go to the journal homepage for more

Download details:

IP Address: 158.227.185.145
This content was downloaded on 20/06/2017 at 11:34

Please note that terms and conditions apply.

You may also be interested in:

Superconducting complementary metasurfaces for THz ultrastrong light-matter coupling
Giacomo Scalari, Curdin Maissen, Sara Cibella et al.

Ultra-strong light-matter coupling for designer Reststrahlen band
B Askenazi, A Vasanelli, A Delteil et al.

Plasmon–terahertz photon interaction in high-electron-mobility heterostructures
Jerzy usakowski

Strong coupling between surface plasmon polaritons and emitters: a review
P Törmä and W L Barnes

Output field-quadrature measurements and squeezing in ultrastrong cavity-QED
Roberto Stassi, Salvatore Savasta, Luigi Garziano et al.

Exciton-polariton trapping and potential landscape engineering
C Schneider, K Winkler, M D Fraser et al.

The impact of microcavity wire width on polariton soliton existence and multistability
G Slavcheva, M V Koleva and A Pimenov

Quantum simulation with interacting photons
Michael J Hartmann

IOP Publishing New J. Phys. 19 (2017) 043022 https://doi.org/10.1088/1367-2630/aa6a2e

New Journal of Physics
The open access journal at the forefront of physics

Deutsche Physikalische Gesellschaft DPG
IOP Institute of Physics

Published in partnership with: Deutsche Physikalische Gesellschaft and the Institute of Physics

OPEN ACCESS

RECEIVED
14 December 2016

REVISED
20 March 2017

ACCEPTED FOR PUBLICATION
30 March 2017

PUBLISHED
19 April 2017

Original content from this work may be used under the terms of the Creative Commons Attribution 3.0 licence.

Any further distribution of this work must maintain attribution to the author(s) and the title of the work, journal citation and DOI.

PAPER

Asymmetry in polariton dispersion as function of light and matter frequencies in the ultrastrong coupling regime

Curdin Maissen[1,2], **Giacomo Scalari**[2], **Mattias Beck and Jérôme Faist**

Institute for Quantum Electronics, ETH Zürich, 8093 Zürich, Switzerland

[1] Current address: Nanooptics group, CIC NanoGUNE, 20018 San Sebastian, Spain.

[2] Author to whom any correspondence should be addressed.

E-mail: cmaissen@nanogune.eu **and** scalari@phys.ethz.ch

Keywords: ultrastrong coupling, terahertz, microcavity, split ring resonator, scaling, LC-resonance, cyclotron

Abstract

In the ultrastrong light–matter coupling regime, non-perturbative effects are observed even for large detuning of the light and matter frequencies. In this regime, the rotating wave approximation breaks down and the contributions of counter-rotating and diamagnetic terms lead to significant spectral modifications. Using split ring resonators coupled to the cyclotron transition in a two dimensional electron gas, we show that the diamagnetic terms lead to an asymmetry between the light and matter branches. Our system allows tuning both, the cavity and the matter frequency over more than two octaves. We find, that the assumption of constant coupling rate Ω as function of detuning is not generally valid for the large frequency range relevant to ultrastrong coupling phenomena.

When the coupling rate Ω between light and matter excitations is similar or larger than the bare frequencies ω_C and ω_0 respectively, the ultrastrong coupling regime is attained [1]. Peculiar predictions for this regime of $\Omega/\omega_r \gtrsim 0.5$ (where ω_r denotes the resonant condition $\omega_C = \omega_0$) encompass the superradiant Dicke quantum phase transition for a critical coupling rate of $\Omega/\omega_r = 0.5$ [2, 3] and decoupling of light and matter for $\Omega/\omega_r > 1$ [4]. New experimental tools [5, 6] could enable in the future the detection of predicted emission of non-classical two-mode squeezed radiation under fast modulation of the coupling rate.

The large fractional coupling rate invalidates the rotating wave approximation. Because the interaction effectively extends over a large frequency range, counter-rotating interaction terms and quadratic diamagnetic terms lead to significant contribution to the interaction energy. These terms have been shown to lead to the renormalization of the polariton frequencies which results in the opening of a polaritonic gap and asymmetric splitting for the lower and upper polariton branches respectively [7–10].

It has been shown theoretically that the presence of the renormalizing A^2-terms prevents the superradiant phase transition [11]. The absence of A^2-terms in various systems [12, 13] and even the elimination thereof [14] has been predicted. To our knowledge, no system in thermodynamic equilibrium, lacking the A^2-term has been realized so far experimentally[3].

Here we report measurements of the polariton dispersion in the ultrastrong coupling regime as function of the detuning of both the cavity and matter frequencies. We observe an asymmetry of the interaction energies when interchanging the cavity and matter frequencies. On the basis of the Hopfield Hamiltonian we explain this asymmetry as a consequence of the A^2-terms which do only act on the light fraction of the polaritons. Moreover, we compare our results to published results in literature to demonstrate that in general Ω cannot be assumed to be constant over the full range of detuning relevant to ultrastrong coupling phenomena.

We use the near-field of the LC-mode of a split ring resonator (SRR) as THz-cavity and couple it to the inter-Landau-level transition ω_0 (cyclotron transition) in a two dimensional electron gas (2DEG) [9]. In this system we can easily tune both the light and matter transition frequencies over more than two octaves (0.2–1 THz). The cyclotron transition frequency is controlled via a perpendicular external magnetic field B_0 following $\omega_0 = \frac{eB_0}{m^*}$,

[3] An exception are driven-dissipative systems [26].

© 2017 IOP Publishing Ltd and Deutsche Physikalische Gesellschaft

where $m^* = 0.069m_e$ is the effective electron mass, e and m_e the free electron charge and mass respectively. In order to modify the LC-mode frequency, we used lithographic tuning.

The paper is organized as follows: first, we report the polariton dispersion for the two cases of fixed light frequency and fixed matter frequency respectively. We will then discuss how the A^2-term leads to the observed asymmetry and show that the frequency dependence of the coupling rate Ω can mask and modify this asymmetry.

Changing the cavity size does generally also change the coupling rate Ω. In the present case of a continuous two dimensional distribution of electrons very close to the plane of the SRR, the coupling rate can be expressed as [9, 15]

$$\Omega = \sqrt{\frac{\lambda_C S_e}{4\pi V_e}}\sqrt{\alpha\nu}\,\omega_0, \tag{1}$$

where $\lambda_c = \frac{2\pi c}{\omega_C}$ is the free space wavelength corresponding to the cavity resonance frequency, $V_e = \int \epsilon_r(\vec{r})|\vec{E}_n(\vec{r})|^2 \mathrm{d}V$ is the effective mode volume with $\vec{E}_n = \frac{\vec{E}}{\max_S(|\vec{E}|)}$ the electric field normalized by its maximal value in the plane of the 2DEG. ϵ_r is the local dielectric function. The effective mode area S_e is used to simplify the effective number of coupled electrons $N_e = \int E_{n+}\mathrm{d}S\frac{\rho_{2\mathrm{deg}}}{\nu} \equiv S_e\frac{\rho_{2\mathrm{deg}}}{\nu}$, where $E_{n+} = \frac{E_x + \mathrm{i}E_y}{2\max_S(|\vec{E}|)}$ is the normalized, cyclotron active polarized electric field and the integral is taken over the plane of the 2DEG. $\nu = \rho_{2\mathrm{deg}}\frac{h}{eB_0} \propto \frac{1}{\omega_0}$ denotes the number of filled Landau levels, and $\alpha = \frac{e^2}{4\pi\epsilon_0\hbar c}$ the fine structure constant. The first square root term of equation (1) accounts for geometric and spectral properties of the cavity mode while the remaining terms result from the electric dipole moment of the cyclotron transition. This latter term is proportional to $\sqrt{\omega_0}$.

An array of complementary metallic SRRs [9, 16] was deposited using standard UV-photo-lithography, electron-beam evaporation, and lift-off technique on a MBE-grown GaAs/$Al_{0.3}Ga_{0.7}As$ heterostructure containing a triangular quantum well 100 nm below the surface. The metal layer consists of a 5 nm Cr adhesion layer, 235 nm Cu, and a 20 nm Au layer for oxidation protection. The resonator dimensions and the simulated electric field distribution of the LC-mode at $\omega_C = 480$ GHz are reported in figure 1(a). The transmission of the structure was measured for a series of applied magnetic field amplitudes B_0 at $T = 3$ K using a time domain spectrometer with normal incidence on the sample surface.

In the transmission spectrum of complementary resonators, the eigenmodes of the coupled light–matter system appear as transmission peaks. Their frequencies were extracted using Lorentzian fit functions and are reported as black dots in figure 1(b). Solid black lines are the best fit of the Hopfield Hamiltonian [15, 17] to the extracted polariton frequencies with the normalized coupling rate $\Omega_r/\omega_r = 0.23$ as fit parameter (with $\omega_r = \omega_C = 480$ GHz). Ω_r denotes the value of the coupling rate at resonance ($\omega_C = \omega_0 \equiv \omega_r$) and corresponds to half of the minimal mode-splitting. We used $\Omega \propto \sqrt{\omega_0}$ in the fit function as stated by equation (1). The best fit was achieved by the least square method (analogously to what was done in [7]) with a normalized rms deviation of 2%.

A polaritonic gap $\Delta\omega_p$ opens between the low magnetic field limit of the upper polariton and the high field limit of the lower polariton. This gap resembles the reststrahlenband for the interaction of light with transverse optical phonons [18] and the gap observed in the interaction with bulk excitons [17]. Here, it does arise from the renormalization of the polariton energy by the diamagnetic terms (A^2 in Hopfield Hamiltonian) and demonstrates that the ultrastrong coupling leads to modifications of the eigenfrequencies even for large detunings $\Delta = \omega_C - \omega_0 \gtrsim \omega_r$.

For the lithographic tuning of the LC-mode frequency we linearly scaled all in-plane dimensions of the SRR by a factor a while keeping the metal thickness constant at 250 nm. Figure 2(a) shows scanning electron micrographs of the largest and smallest resonator structure with $a = 2.4$ and $a = 0.5$ respectively. The electromagnetic mode profile in the out-of-plane direction is independent of the film thickness, due to the quasi two dimensional nature of the SRR. Consequently, the scaling of the in-plane dimensions results in isotropic scaling of the electromagnetic near-field distribution in all three spatial dimensions. In accordance to the scale invariance of Maxwell equations, the LC-mode frequency follows an a^{-1} dependence as shown by the measurements in figure 2(a). The cavity frequencies were extracted from the lower polariton frequency in the high magnetic field limit. The lower polariton approaches the unloaded cavity frequency in the Hopfield model.

With this result, we can estimate the dependence of the geometric factor given by the first square root term in equation (1) on the scaling parameter a. For linear in-plane scaling of the SRR dimensions is $V \propto a^3$, and $\lambda \propto a$ as found above with the measurements of the empty resonator frequencies. For a distance between the 2DEG and the SRR layer which is much smaller than any lateral dimensions of the SRR, the effective area scales directly as $S_e \propto a^2$. In the present case thus, one expects Ω to be constant as function of ω_C.

We verified these scaling properties by measuring Ω_r as function of the scaling parameter a. Ω_r was exctracted as described above by fitting polariton dispersion as function of magnetic field with the Hopfield

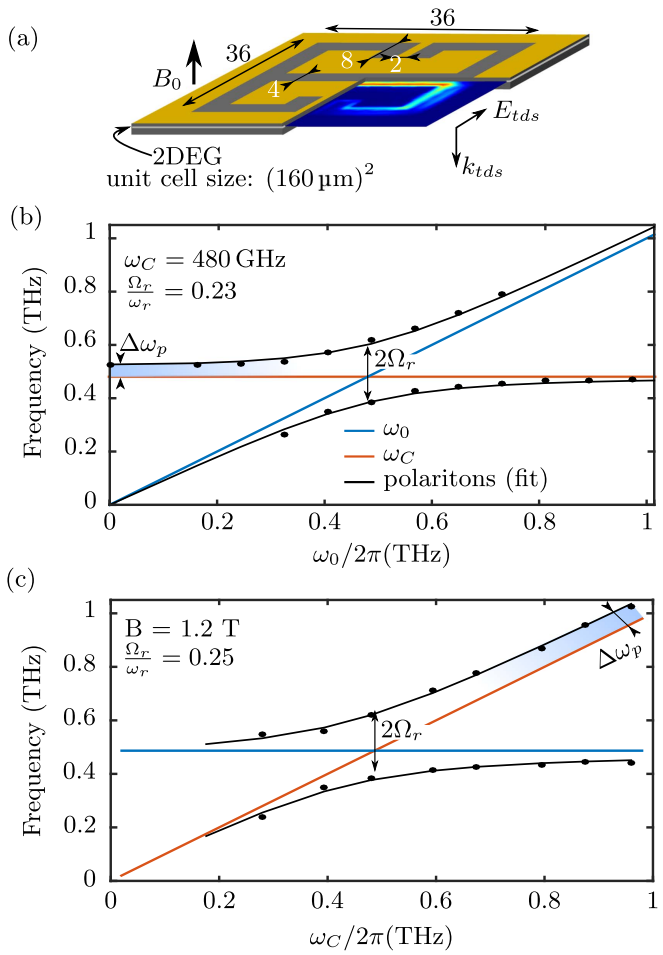

Figure 1. (a) Schematic of the SRR array deposited on top of a 2DEG with dimensions given in μm. The static magnetic field B_0 is applied perpendicular to the 2DEG plane and the spectrometer electric field $E_{\rm tds}$ is polarized perpendicular to the middle gap of the SRR structure. The overlay in the front right corner is the simulated electric field distribution associated to the LC-mode. (b) Polariton dispersion for fixed cavity frequency ω_C measured as function of ω_0: dots are the polariton frequencies as extracted from measurements. Black lines are best fits of the Hopfield-model using Ω_r/ω_r as fitting parameter. Straight lines indicate the bare cavity and matter frequency respectively. The polaritonic gap $\Delta\omega_p$ which opens along the light branch is shaded in blue. (c) Polariton dispersion for fixed matter frequency $\omega_0 = 2\pi \times 485$ GHz ($B = 1.2$ T) and lithographic tuning of the cavity frequency. A gap opens also in this case between the bare cavity frequency and the upper polariton branch in the limit of $\omega_C > \omega_0$.

Hamiltonian. The resulting normalized coupling rates Ω_r/ω_r are reported in figure 2(b), plotted as function of $\sqrt{\nu} \propto 1/\sqrt{\omega_0}$. The solid line is a linear fit to the normalized coupling rate from which follows that $\Omega_r \propto \frac{\omega_r}{\sqrt{\omega_0}}$. This scaling is in agreement with the scaling of $\Omega \propto \sqrt{\omega_0}$ expected from equation (1) since the scaling was determined at resonance with $\omega_0 = \omega_C \equiv \omega_r$. The small deviations observed for small cavity dimensions are probably due to the fact, that the gap size of the SRR becomes comparable to the spacing between the SRR and 2DEG planes.

The transmission spectrum for all nine samples at fixed magnetic field $B = 1.2$ T are plotted in figure 3 showing clear mode splitting (dashed lines are a guide to the eye). For large detuning $\Delta = \omega_C - \omega_0$ the matter like branch disappears.

The transmission peak frequencies are plotted in figure 1(c) as function of the cavity frequency. Comparing the position of the polaritonic gap with the case displayed in figure 1(b) shows clearly the asymmetry when tuning the light or matter frequency respectively.

The polariton frequencies are given by the solutions of the secular equation [15]

$$0 = \omega^4 - \omega^2(\omega_0^2 + \omega_C^2) + \omega_C^2\omega_0^2 - 4D\omega_C(\omega^2 - \omega_0^2) - 4\Omega^2\omega_C\omega_0 \tag{2}$$

$$= \omega^4 - \omega^2(\omega_0^2 + \omega_C^2) + \omega_C^2\omega_0^2 - 4\Omega^2\omega^2\frac{\omega_C}{\omega_0}. \tag{3}$$

D denotes here the diamagnetic interaction rate arising from the A^2 terms in the minimal coupling Hamiltonian. In the second equation, we replaced $D = \frac{\Omega^2}{\omega_0}$ [1, 15] (assuming unity oscillator strength of the electronic transition). Note, that equation (2) is symmetric in ω_C and ω_0 for $D = 0$.

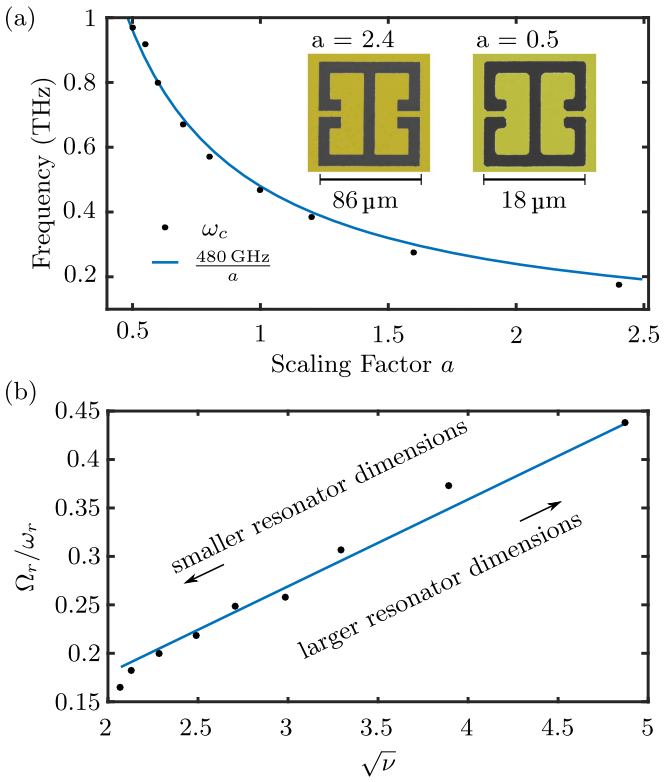

Figure 2. (a) LC-mode frequency as function of the scaling parameter a following the expected inverse proportionality which is indicated by the solid line. Insets show false-colored SEM pictures of the largest and smallest SRR. (b) Normalized coupling rates at resonance ($\omega_0 = \omega_C \equiv \omega_r$) for the nine resonator dimensions plotted against the filling factor $\sqrt{\nu}$. The linear behavior indicates that the geometric factor in equation (1) remains constant for different resonator dimensions.

In general, the polariton dispersion is modified by any frequency dependence of the coupling rate Ω. For the case of linearly scaled SRRs coupled to the cyclotron transition of a continuous 2DEG, we have found $\Omega \propto \sqrt{\omega_0}$. In contrast, for intersubband-transitions with which ultrastrong coupling has been demonstrated first [21], $\Omega \propto \sqrt{\frac{\omega_0}{\omega_C}}$ is found for patch cavities [22]. The scaling with $1/\sqrt{\omega_C}$ is a consequence of the fact that the ratio N_e/V remains constant in double metal cavities, while $N_e/V \propto \omega_C$ for the SRR. This ratio does actually reflect the field overlap of the photonic mode with the electronic excitations.

To illustrate the effect of these different scaling properties on the polariton dispersion, we compare in figure 4(a) the dispersion for our system with published results for double metal LC-resonators coupled to the intersubband transition of parabolic quantum wells [20]. Data is plotted in normalized units, were we used the frequency reached by the lower polariton in the limit $\omega_C \gg \omega_0$ as normalization frequency ($\omega_r = 2\pi \times 3.66$ THz for the double metal cavity data). This choice for the scaling allows to describe both systems with the Hopfield Hamiltonian [22] whose results are given by the solid and dashed lines respectively. The difference resembles the asymmetry between figures 1(b) and (c). However, while the difference in figure 1 arise from both, the asymmetry introduced by the A^2-terms and frequency dependence of Ω, the different polariton dispersion in figure 4(a) arises from differing frequency dependence of Ω alone.

The scaling properties of SRRs and double metal resonators are illustrated in figure 4(b). The overlap factor (i.e. N_e/V) does in general not change for double metal resonators, and thus $\Omega \propto 1/\sqrt{\omega_C}$ is independent of the actual resonator geometry. For more general approaches to the scaling of the cavity frequency (i.e. isotropic scaling or scaling of parts only), the coupling rate might also take the form of a more complicated function of ω_C [23, 24].

The asymmetry between light and matter branches arises from the ratio $\frac{\omega_C}{\omega_0}$ in equation (3). The cavity frequency ω_C enters this ratio, because the renormalization terms act on the photonic part only. The factor $1/\omega_0$ which is introduced by the expression for $D \propto 1/\omega_0$ leads to divergent solutions when the matter frequency approaches zero while keeping Ω constant. Moreover, the asymmetry given by the fraction ω_C/ω_0 would be lifted for a system with $\Omega \propto \omega_C^x \omega_0^{x+1}$. Note, that the polariton frequencies for $\omega_C = \omega_0$ are independent of the scaling properties of Ω and also the minimal mode splitting is always found for $\omega_C = \omega_0$ in systems described by the Hopfield Hamiltonian.

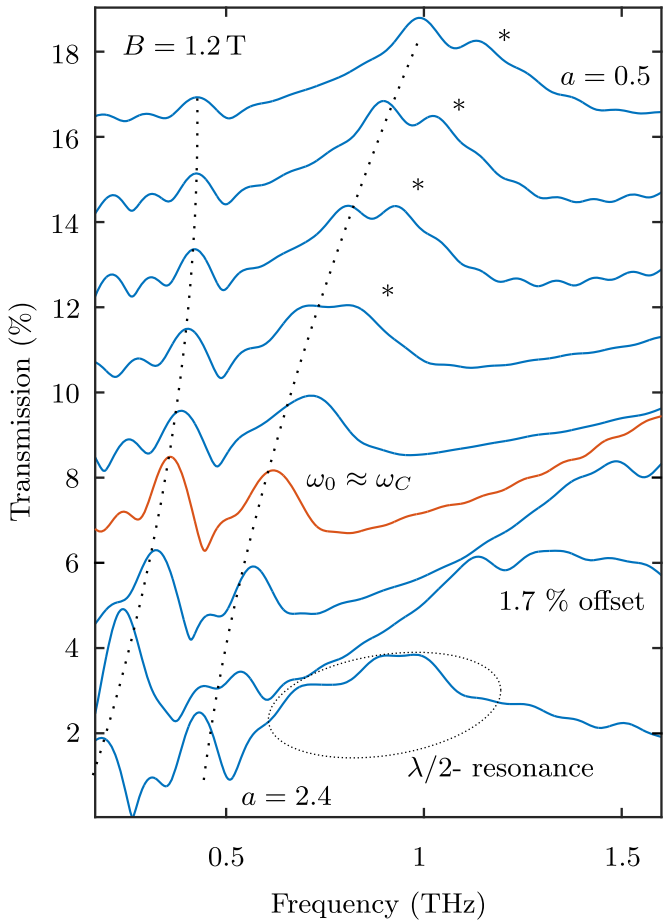

Figure 3. Transmission spectra for varying scaling parameter a at constant matter frequency $\omega_0 = 2\pi \times 485$ GHz($B = 1.2$ T). The cyclotron like polariton disappears for large detunings (spectra offset by 1.7% for clarity, dashed lines are a guide to the eye). Asterisks indicate plasmonic resonances arising from the periodicity of the SRR array [19]. For the large resonator structures lies also the broad $\lambda/2$ inside the spectral range of the experiment.

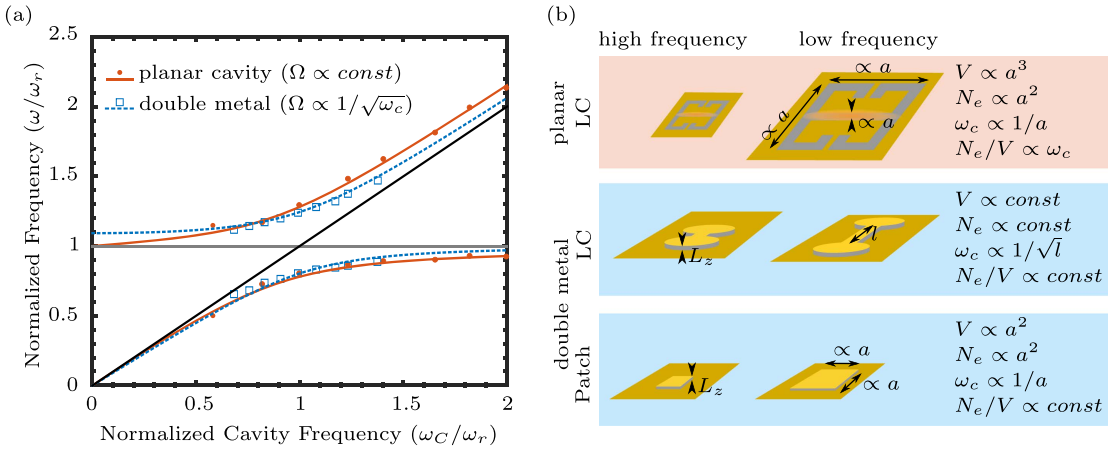

Figure 4. (a) Comparison of the measurements already reported in figure 1(c) (orange dots) and the case of the intersubband transition coupled to double metal LC-resonators (blue squares, data from [20]). They follow the corresponding calculated dispersion curves which differ in the normalized coupling rates ($\Omega_r/\omega_r = 0.25$ for SRR versus $\Omega_r/\omega_r = 0.22$ for double metal LC-resonators) and in the scaling of the coupling rate with frequency. (b) Illustration of the scaling behavior of SRRs and double metal LC-resonators: linear in-plane scaling of the SRR leads to an effective 3D scaling of the electric field distribution due to the proportionality of the out-of-plane confinement with the size of the openings. In contrast, for double metal cavities, the scaling is at most 2D, the case realized with patch cavities (L_z is constant and given by the heterostructure). For double metal LC- cavities, the electric field mode volume remains constant if only the inductive part is scaled. In either case, for double metal cavities the change in mode volume is compensated by the change in the number of coupled electronic states and the ratio N_e/V remains constant as a function of cavity frequency.

In conclusion, we have presented new experimental results showing how the presence of the diamagnetic renormalization terms in the Hopfield Hamiltonian leads to an asymmetric polaritonic dispersion as function of the cavity and matter frequencies respectively. Analyzing the characteristic equation for the full Hamiltonian including counterrotating and diamagnetic terms, we found that the asymmetry arises due to the action of the diamagnetic term on the cavity fractions only, and due to its proportionality with the inverse matter frequency $1/\omega_0$. Moreover, comparing our results with published data, we have crystalized the fact, that the assumption of constant coupling rate Ω as function of detuning is generally not fulfilled. It depends on the actual cavity geometry and has to be determined through microscopic calculations [9, 22, 25]. This finding is particularly relevant to microcavities, where changes in frequency imply significant changes in the cavity geometry and possibly in the mode overlap.

Acknowledgments

This research was supported by the Swiss National Science Foundation (SNF) through the National Centre of Competence in Research Quantum Science and Technology (QSIT) and through the SNF Grant No. 129823, and by the ERC Advanced Grant *Quantum Metamaterials in the Ultra Strong Coupling Regime (MUSiC)*. We acknowledge the support by the FIRST clean room FOT and helpful discussion with Janine Keller.

References

[1] Ciuti C, Bastard G and Carusotto I 2005 *Phys. Rev.* B **72** 115303
[2] Hepp K and Lieb E H 1973 *Ann. Phys., NY* **76** 360
[3] Wang Y K and Hioe F T 1973 *Phys. Rev.* A **7** 831
[4] De Liberato S 2014 *Phys. Rev. Lett.* **112** 016401
[5] Riek C, Seletskiy D, Moskalenko A, Schmidt J, Krauspe P, Eckart S, Eggert S, Burkard G and Leitenstorfer A 2015 *Science* **350** 420
[6] Benea-Chelmus I-C, Bonzon C, Maissen C, Scalari G, Beck M and Faist J 2016 *Phys. Rev.* A **93** 043812
[7] Anappara A A, De Liberato S, Tredicucci A, Ciuti C, Biasiol G, Sorba L and Beltram F 2009 *Phys. Rev.* B **79** 201303
[8] Scalari G *et al* 2012 *Science* **335** 1323
[9] Maissen C, Scalari G, Valmorra F, Beck M, Faist J, Cibella S, Leoni R, Reichl C, Charpentier C and Wegscheider W 2014 *Phys. Rev.* B **90** 205309
[10] Zhang Q, Lou M, Li X, Reno J L, Pan W, Watson J D, Manfra M J and Kono J 2016 *Nat. Phys.* **12** 1005–11
[11] Rzażewski K, Wódkiewicz K and Żakowicz W 1975 *Phys. Rev. Lett.* **35** 432
[12] Hagenmüller D and Ciuti C 2012 *Phys. Rev. Lett.* **109** 267403
[13] Baksic A, Nataf P and Ciuti C 2013 *Phys. Rev.* A **87** 023813
[14] Vukics A, Grießer T and Domokos P 2014 *Phys. Rev. Lett.* **112** 073601
[15] Hagenmüller D, De Liberato S and Ciuti C 2010 *Phys. Rev.* B **81** 235303
[16] Chen H-T, O'Hara J F, Taylor A J, Averitt R D, Highstrete C, Lee M and Padilla W 2007 *Opt. Express* **15** 1084
[17] Hopfield J J 1958 *Phys. Rev.* **112** 1555
[18] Ashcroft N W and Mermin D 2008 *Solid State Physics* (Belmon: Brooks/Cole)
[19] Keller J *et al* 2017 *Adv. Opt. Mater.* **5** 1600884
[20] Geiser M, Castellano F, Scalari G, Beck M, Nevou L and Faist J 2012 *Phys. Rev. Lett.* **108** 106402
[21] Günter G *et al* 2009 *Nature* **458** 178
[22] Todorov Y and Sirtori C 2012 *Phys. Rev.* B **85** 045304
[23] Dietze D, Unterrainer K and Darmo J 2013 *Phys. Rev.* B **87** 075324
[24] Maissen C *et al* 2013 *Proc. SPIE 8623, Ultrafast Phenomena and Nanophotonics XVII, 86231M (March 14, 2013)* (https://doi.org/10.1117/12.2004328)
[25] Askenazi B, Vasanelli A, Delteil A, Todorov Y, Andreani L, Beaudoin G, Sagnes I and Sirtori C 2014 *New J. Phys.* **16** 043029
[26] Baumann K, Guerlin C, Brennecke F and Esslinger T 2010 *Nature* **464** 1301